NJC

Accepted Manuscript

This is an *Accepted Manuscript*, which has been through the Royal Society of Chemistry peer review process and has been accepted for publication.

Accepted Manuscripts are published online shortly after acceptance, before technical editing, formatting and proof reading. Using this free service, authors can make their results available to the community, in citable form, before we publish the edited article. We will replace this *Accepted Manuscript* with the edited and formatted *Advance Article* as soon as it is available.

You can find more information about *Accepted Manuscripts* in the Information for Authors.

Please note that technical editing may introduce minor changes to the text and/or graphics, which may alter content. The journal's standard Terms & Conditions and the Ethical guidelines still apply. In no event shall the Royal Society of Chemistry be held responsible for any errors or omissions in this *Accepted Manuscript* or any consequences arising from the use of any information it contains.

ROYAL SOCIETY OF CHEMISTRY

www.rsc.org/njc

Embryonic ZSM-5 zeolites: Zeolitic materials with superior catalytic activity in 1,3,5-triisopropylbenzene dealkylation

Kok-Giap Haw,[a] Jean-Michel Goupil,[a] Jean-Pierre Gilson,[a*] Nikolai Nesterenko,[b] Delphine Minoux,[b] Jean-Pierre Dath,[b] Valentin Valtchev,[a]

[a]*Laboratoire Catalyse et Spectrochimie, ENSICAEN, Université de Caen, CNRS, 6 Boulevard Maréchal Juin, 14050 Caen, France; E-mail: jean-pierre.gilson@ensicaen.fr*
[b]*Total Research and Technology Feluy (TRTF), Zone Industrielle C, 7181 Feluy, Belgium*

Abstract

Embryonic ZSM-5's are harvested from clear ZSM-5 precursor solutions after freeze-drying and calcination. These materials are microporous with pore sizes close to those of ZSM-5 zeolites. Due to their partially formed structure, embryonic zeolites do not display long range order and are XRD amorphous. Their micropores are highly accessible, resist to high temperature treatments and the strenght of their acid sites is comparable to zeolites. These characteristics give them superior catalytic performances in the conversion of a bulky model molecule, 1,3,5-triisopropylbenzene.

Keywords: Embryonic zeolite, ZSM-5 precursor, microporous, amorphous.

Introduction

The discovery of ZSM-5 (MFI structure type) stimulated much academic research; it belongs now to the "Big Five" zeolites, *i.e.* those produced in significant amount for applications in the field of catalysis.[1, 2] The accessibility of its micropores is however limited by their small opening (*ca.* 0.55 nm), a major drawback in some reactions. Over the last decade, a renewed interest in hierarchical (micro-mesoporous mainly) and nano-sized zeolites allowed to drastically reduce such diffusion constraints in some reactions.[3-13] The inclusion of mesopores in zeolitic materials significantly shortens the diffusion path length of reactants and products,[14] reducing their contact times in the micropore network and improving their overall performances, including deactivation by coke.[15, 16] Six main types of micro-mesoporous materials are currently explored: *i*) nano-sized zeolites (sizes below 100 nm), *ii*) zeolites with intra crystalline mesopores, *iii*) zeolite composites on various mesoporous supports, *iv*) ordered

mesoporous materials assembled from zeolitic nano particles, *v*) 2D zeolites, and *vi*) zeolite nano-sheets.

The last frontier in such a family of materials would be partially formed or more open zeolitic structures with a larger proportion of their active sites accessible. Earlier attempts are described in the literature on "organizing a short-range order" in amorphous aluminosilicates[17, 18] or stopping the crystallization of classical micron-sized zeolites.[19] We describe in this contribution a new general method for the preparation of materials called "embryonic zeolites". It is based on a gel composition yielding nano-sized ZSM-5, modified to produce an embryonic zeolite. Such a synthesis is carefully controlled by shortening the synthesis time commonly required for the preparation of nano-zeolite crystals (< 100 nm). The resulting partially-formed structures will not possess long-range order and their more open micropores will provide shorter and easier diffusion pathways. These features concur to improve mass transfer and should lead to better catalysts, especially in the processing of bulky molecules, if their acidic properties (number and strength) are not too degraded with respect to zeolites. To that end, two types of materials are prepared, characterized and evaluated in the catalytic dealkylation of a bulky molecule, 1,3,5-triisopropylbenzene:

i) embryonic zeolites prepared at room temperature

ii) the materials described above further treated under hydrothermal conditions to increase the number of embryos while avoiding crystallization.

Experimental

Synthesis

Embryonic ZSM-5 zeolites are synthesized from a precursor solution of this zeolite with different SiO_2 and Al_2O_3 compositions. A typical synthesis procedure is as follows: a Tetrapropylammonium hydroxide (TPAOH 20% in water, Alfa Aesar) solution, distilled water, aluminum sulfate (98%, Aldrich), and Tetraethylorthosilicate (TEOS 98%, Aldrich) are mixed to obtain a series of clear solutions with the following compositions: 4.5 $(TPA)_2O$: y Al_2O_3: 25 SiO_2: 430 H_2O: 100 EtOH, where y = 0.0625 to 0.50. After mixing, hydrolysis takes place at room temperature (RT) for 4 h in a closed bottle. Complete hydrolysis is confirmed when a monophasic clear solution appears. Freeze drying is selected, rather classical drying, to avoid any crystallization at this

stage. The clear solution is frozen by immersing the sample in liquid nitrogen; freeze-drying takes place at -90°C under vacuum. The dried samples are then calcined under air at 550°C (100°C/h) to obtain the H-form of embryonic zeolite. The resulting materials are referred to as RT-n, where n is the SiO_2/Al_2O_3 molar ratio of the starting gel.

To increase the number of embryos and increase their thermal stability, the best (based on its catalytic performance, *vide infra*) of the above-prepared materials, RT-100, is subjected to additional hydrothermal treatments. Clear homogeneous precursor solutions of RT-100 are sealed in Teflon lined-stainless steel autoclaves kept at 100°C in an oven under quiescent conditions for various times (12–29 h) and then cooled to room temperature. The solid phases are recovered by freeze drying, then calcined under air at 550°C (100°C/h), *vide infra,* for characterization and catalytic testing. The hydrothermally treated precursors are labeled HT-100-x, with x=hydrothermal treatment time (h); RT-100 is therefore equivalent to HT-100-0.

Characterization

The materials are first characterized by X-ray diffraction (XRD) with a PANalytical X'Pert Pro diffractometer using a Cu K_α radiation (λ = 1.5418 Å) in the 2θ range 3-50º (step size of 0.02º). Electron micrographs are recorded on a TESCAN Mira scanning electron microscope (SEM) operating at 30 kV. To improve the electrical conductivity of the sample and avoid charging, the samples are sputtered with platinum. Nitrogen adsorption is measured on a Micromeritics ASAP 2020 surface area analyzer. The calcined samples are analyzed after degassing at 300°C. The isotherms are recorded and processed using the ASAP 2020 analysis software; micropore volume (V_{mic} / cm^3 g^{-1}) and external surface area (S_{ext} / m^2 g^{-1}) are obtained from the t-plot using the Harkins-Jura equation[20]:

$$\frac{t}{nm} = 0.1\left(\frac{13.99}{0.034 - \log\left(\frac{P}{P^\circ}\right)}\right)^{0.5}$$

The size (diameter) distribution of the mesopores is obtained from the desorption branch of the isotherm using the Barrett Joyner Halenda (BJH) model[21] assuming cylindrical pores. The micro-mesopores size distribution is obtained from a density functional theory (DFT) modelling[22-24] of the adsorption branch (parameterization: N_2

gas, cylindrical pores, oxide surface, and medium regularization). Particles size is measured by dynamic light scattering (DLS) on a Malvern ZetaSizer Nano Series. Before loading the samples in the cells, the samples are stabilized in water at 25°C.

The solid-state magic angle spinning nuclear magnetic resonance (MAS NMR) measurements are performed on a Bruker Advance 500 spectrometer using 4 mm zirconia rotors. The ^{27}Al chemical shifts are determined using a 1M aqueous $Al(NO_3)_3$ reference solution and the spectra acquired under the following conditions: $\pi/12$ pulse and recycle delay of 1 s. Deconvolution and fitting of the NMR spectra are performed using the *dmfit* program.

Catalytic tests

The catalytic performance, of the protonic form of the materials harvested, are evaluated in the dealkylation of a model bulky molecule, 1,3,5-triisopropylbenzene (TiPBz). TiPBz is commonly used to study the catalytic properties of the external surface of zeolites because its kinetic diameter, 0.95 nm, is well above the pore openings of any of conventional aluminosilicate zeolites. In a typical catalytic test, 20 mg of catalyst is loaded at the center of a stainless steel tubular reactor (internal diameter of 1/2") and activated *in-situ* for 1 hour at 460°C (ramping from room temperature at 5°C/min) under an air flow (50 $ml{\cdot}min^{-1}$). After this activation, the temperature is decreased to 300°C, the reaction temperature, under a N_2 flow. TiPBz is fed to the reactor by diverting a nitrogen flow (200 $ml{\cdot}min^{-1}$) to a saturator held at 70°C and filled with TiPBz (Alfa Aesar, 97%), resulting in a constant Weight Hourly Space Velocity (WHSV) of 8 h^{-1} for all the tests. The conversions are measured at 300°C during 180 min. The effluents, transferred via a heated line (150°C) to a gas sampling valve are analyzed online on a Varian CP-3800 Gas Chromatograph equipped with a flame ionization detector (FID) and a HP-PONA cross-linked methyl siloxane column, 50 m (L) x 0.2 mm (ID) x 0.5 µm (film thickness). The column, injection and detector temperatures are set at 160°C, 200°C and 250°C respectively.

Results and discussion

Synthesis of embryonic zeolite at room temperature

All samples harvested are X-Ray amorphous. Nitrogen sorption shows Type I isotherms for the non-hydrothermally treated precursors with SiO_2/Al_2O_3 between 100 and 400 (RT-100, RT-200 and RT-400) (**Figure 1a**). A different isotherm is observed for RT-50 (SiO_2/Al_2O_3=50); the nitrogen uptake after 0.2 P/Po is not horizontal and suggests the presence of mesopores. This is confirmed by the large mesopore distribution (**Figure 1b**). Micropores of different sizes (1-5 nm) are present in all samples as indicated by the multiple steps in the nitrogen uptake (**Figure 1c)**.

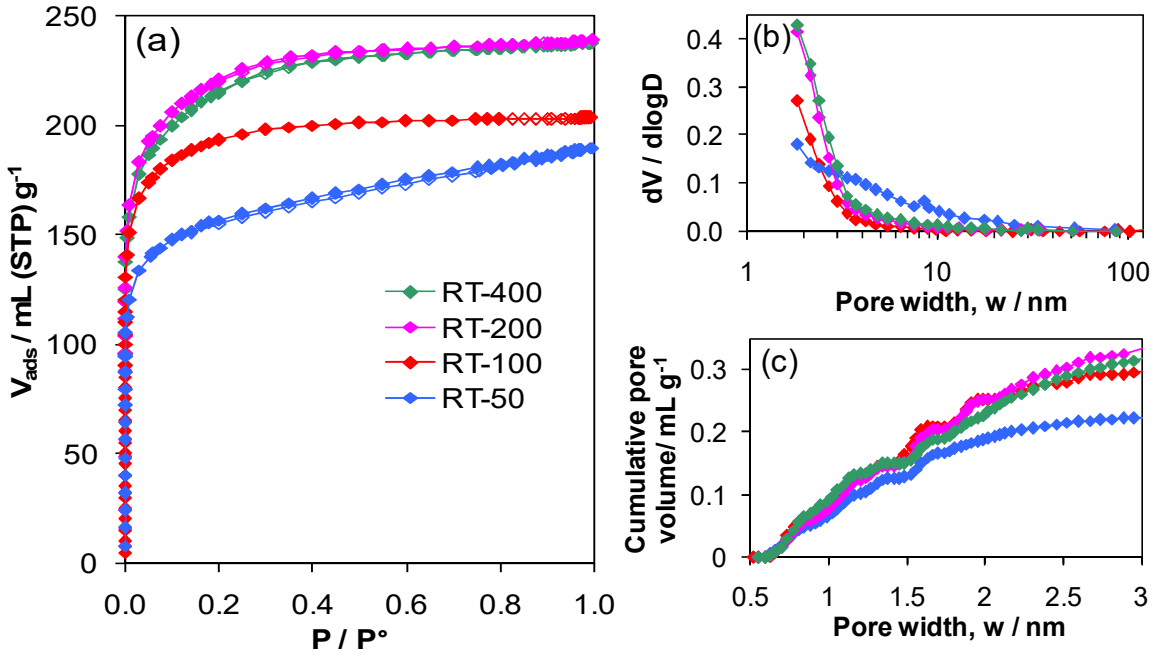

Figure 1: (a) Nitrogen adsorption-desorption isotherms of ZSM-5 precursors, (b) BJH pore size distribution (desorption branch) and (c) cumulative pore volume (DFT).

In general, increasing the SiO_2/Al_2O_3 in the precursor mixture leads to higher surface area and micropore volume (**Table 1)**. Also, all samples exhibit BET surface areas and micropore volumes substantially higher than those of a MFI zeolite.

Table 1: Physical properties of the calcined materials.

Samples	[a]Crystalline	SiO_2/Al_2O_3 mol ratio	S_{BET}/ m^2g^{-1}	[b]S_{EXT}/ m^2g^{-1}	[b]V_{micro}/ cm^3g^{-1}	V_{meso}/ cm^3g^{-1}	V_{Tot}/ cm^3g^{-1}
RT-50	No	50	521	99	0.20	0.09	0.29
RT-100	No	100	640	28	0.29	0.02	0.31
RT-200	No	200	740	44	0.33	0.04	0.37
RT-400	No	400	725	39	0.33	0.04	0.37

[a] by XRD; [b] S_{EXT} and V_{mic} determined from the t-plot.

Rizzo *et al.*,[25] working with a $TPAOH/SiO_2$=0.2, observed that the rate of gelation increases with aluminum content and harvested microporous solids with gel compositions of SiO_2/Al_2O_3=300 and ∞, while micro-mesoporous solids were obtained with SiO_2/Al_2O_3=100. They explained their results by a slower polymerization in the presence of Al, favoring cross-linking and gelation. However, we do not observe such an effect with our gel compositions in the range SiO_2/Al_2O_3=100-400 and harvest only microporous materials. We attribute this result to our higher $TPAOH/SiO_2$ (0.36) and pH (14) promoting hydrolysis and therefore the formation of small precursor units. Increasing the aluminum content to SiO_2/Al_2O_3=50 slows TEOS hydrolysis and increases solution viscosity. This suggests that at a SiO_2/Al_2O_3=50, the stability of the solution approaches its limit and further aluminum addition will lead to gelation.

Figure 2a shows the ^{27}Al MAS NMR spectra of the as-prepared ZSM-5 precursors. Only aluminum in tetrahedral coordination is observed, indicating that the aluminate species fully react with the silicate species present. A more intense signal is detected on the sample with higher aluminum content. **Figure 2b** shows the ^{27}Al MAS NMR spectrum of RT-100 calcined at 550°C under air; most of its aluminum remains tetrahedrally coordinated and only a small amount of octahedral aluminum (~0 ppm) appears after the combustion of organic template.

TEOS hydrolysis can take place in both acidic and basic conditions. However, replacing TPAOH with sulfuric acid in the RT-100 preparation indicates that this promotes TEOS hydrolysis but not its polymerization and aluminum incorporation in a tetrahedral network, **Figure 2c**.

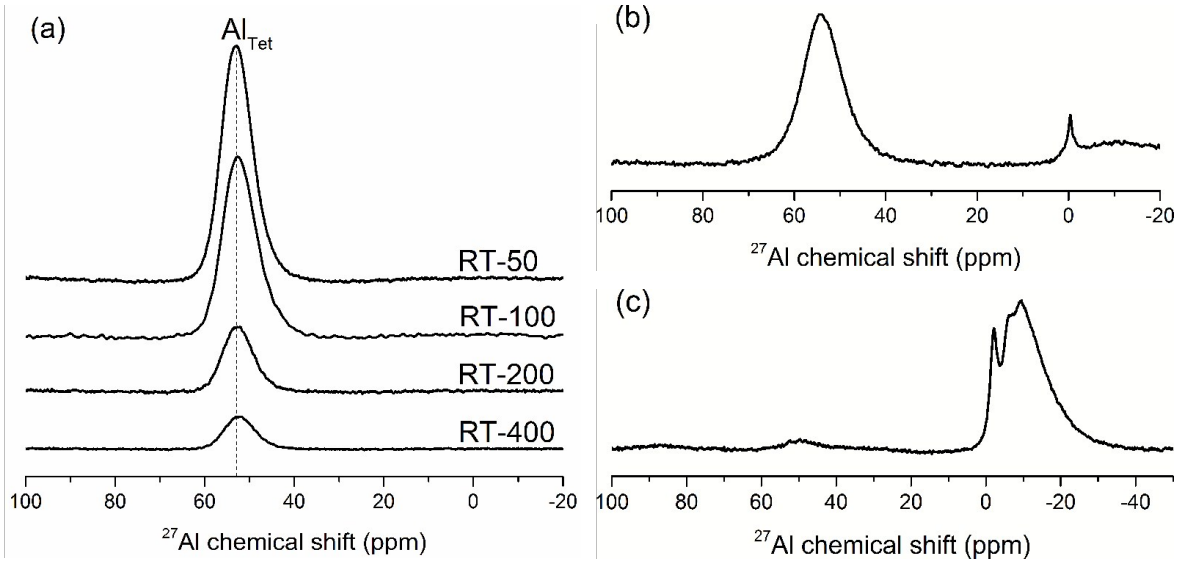

Figure 2: ^{27}Al MAS NMR spectra of (a) as-prepared ZSM-5 precursors, (b) RT-100 calcined at 550°C under air, and (c) RT-100 using sulfuric acid as hydrolyzing catalysts. Note: intensity scales are different for (b) and (c).

The derived catalysts (protonic form, calcination at 460°C) are tested in the de-alkylation of TiPBz (**Figure 3**). There is clearly a maximum in conversion as a function of the SiO_2/Al_2O_3; first an increase from RT-50 to RT-100 followed by a continuous decrease. This is an indication of the possible presence of two competing effects, *i.e. i*) an initial increase of the accessibility of these sites due to the preparation conditions, *ii*) a decrease of the (tetrahedral) aluminum concentration leading to less Brønsted acid sites.

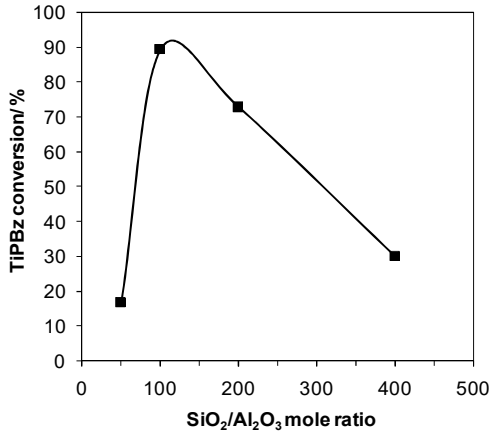

Figure 3: Dealkylation of TiPBz on RT-n catalysts. Conditions: $T_{reaction}$= 300°C, WHSV = 8 h^{-1}, TOS = 2 min.

Synthesis of embryonic zeolite under hydrothermal conditions

To increase the amount of catalytically active embryonic zeolites, RT-100 is further processed under hydrothermal conditions. **Figure 4** shows the DLS particle size distribution of the resulting materials (HT-100-x where x stands for the hydrothermal treatment time).

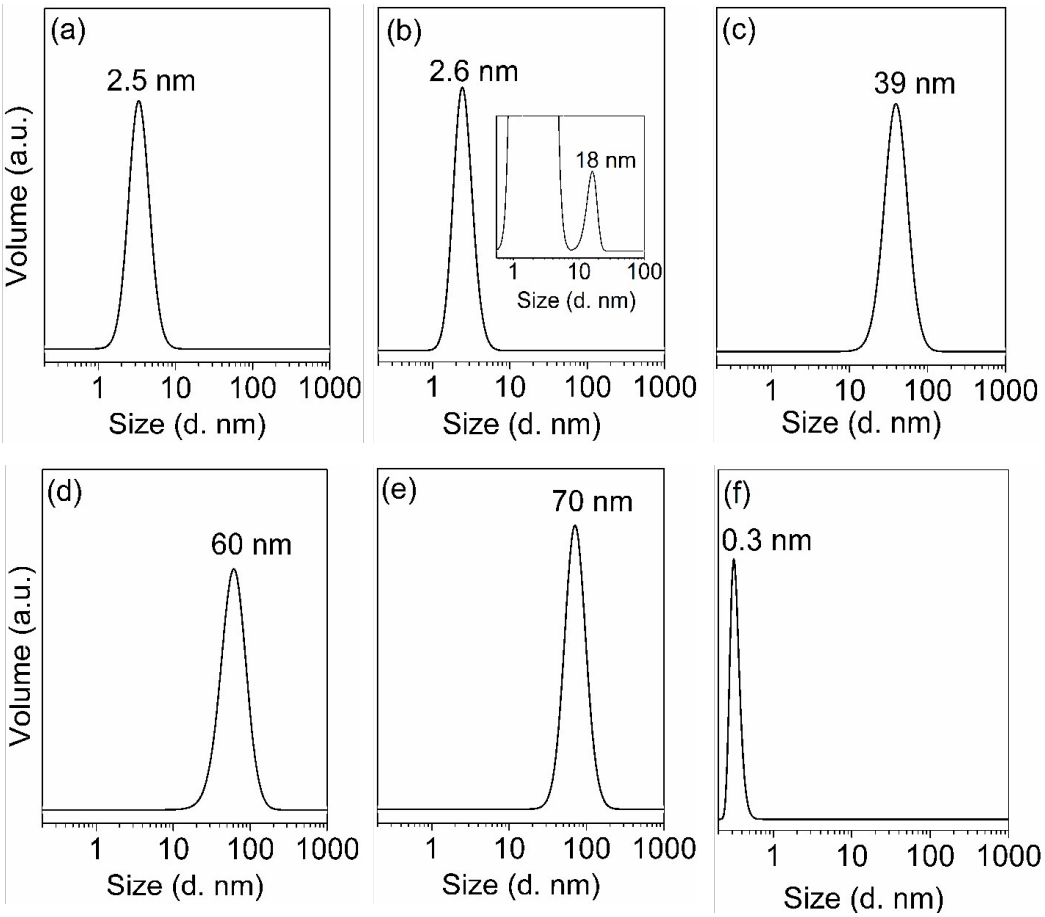

Figure 4: Particle size distribution of (a) RT-100, (b) HT-100-12, (c) HT-100-18, (d) HT-100-24, (e) HT-100-29, and (f) RT-100 with H_2SO_4 as hydrolyzing agent.

A monomodal particle size distribution of 2.5 nm is observed before processing of the gel and during the first 12 h of its hydrothermal treatment. The Al-free (RT-100) sample prepared with H_2SO_4 shows small particles of 0.3 nm, while 2.5 nm particles are formed in the presence of TPAOH. Similar results are reported in the literature using a combination of in situ SAXS, USAXS and WAXS (ultra-small and wide-angle X-ray scattering).[26, 27] Kirschhock *et al.* suggested that these particles are the primary units for

zeolite crystallization and proposed that precursors with dimension of 4×4×1.3 nm already possess the MFI-type topology.[28-31] Previous studies showed that a close interaction between TPA cations and silicate species already takes place before the formation of long-range crystalline structure.

A second population with a size of 18 nm is detected after 12 h of treatment (inset **Figure 4 b**). XRD shows that these particles are growing crystals of zeolite ZSM-5 (**Figure 5**). This population increases in size almost linearly during crystallization and reaches 70 nm after 29 h (**Figure 6a**). SEM confirms the crystal sizes observed by DLS (**Figure 6b**) and shows spherical or slightly elliptical uniform ZSM-5 aggregates. Each aggregate consists of individual nano-crystals of approximately 20 nm. Micropore volumes and specific surface areas increase with crystallization time (**Table 2**); moreover, the micropore volume of X-Ray-amorphous and semi-crystalline samples exceeds substantially the typical micropore volume of MFI-type material (0.18 cm^3g^{-1}). This suggests that the microporosity is more open than on crystalline MFI.

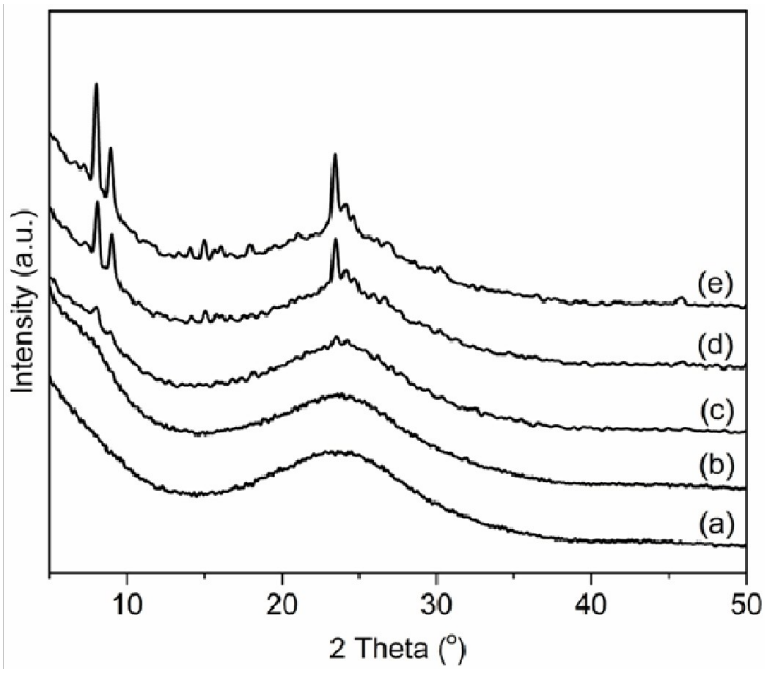

Figure 5: XRD patterns of (a) RT-100, (b) HT-100-12, (c) HT-100-18, (d) HT-100-24, (e) HT-100-29.

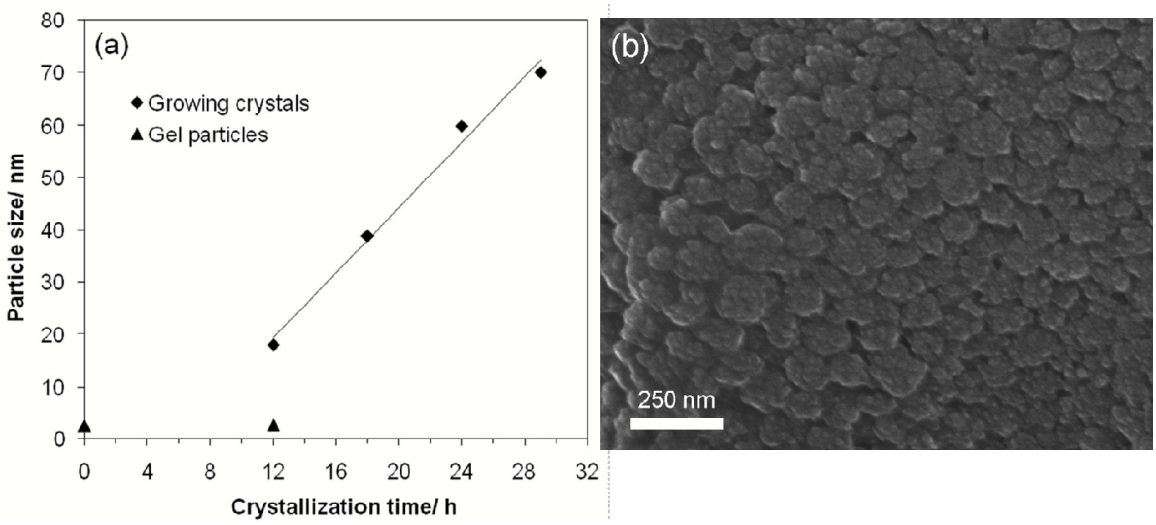

Figure 6: (a) Particle size as a function of crystallization time; (b) SEM micrograph of crystalline ZSM-5 product obtained at 100°C for 29 h.

Table 2: Physical properties of the hydrothermally treated precursors.

Samples	S_{BET}/ m^2g^{-1}	[a] S_{EXT}/ m^2g^{-1}	[a, b] V_{micro}/ cm^3g^{-1}	V_{meso}/ cm^3g^{-1}	V_{Tot}/ cm^3g^{-1}
RT-100	640	9	0.30	0.01	0.31
HT-100-12	627	9	0.31	0.02	0.33
HT-100-18	725	9	0.36	0.01	0.37
HT-100-24	748	15	0.39	0.02	0.41
HT-100-29	772	14	0.39	0.02	0.41

[a] S_{EXT} and V_{mic} determined by t-plot; [b] Total micropore volume of (amorphous phase) in RT-100 and (amorphous/crystalline phases) in hydrothermally treated (HT-100) samples.

Catalytic test

Catalysts derived from the semi crystalline silica-alumina materials are again tested in the de-alkylation of TiPBz (**Figure 7a**). Hydrothermally treated (HT) amorphous precursors show higher catalytic activity than solids already containing some crystalline ZSM-5. Both DLS and XRD measurements show that 18 nm ZSM-5 crystals are present in HT-100-12, *i.e.* after 12 h of hydrothermal treatment. The material obtained after 18 h of hydrothermal treatment (HT-100-18) displays the highest catalytic activity. After 18 h of hydrothermal treatment, the conversion decreases while the XRD crystallinity and the DLS particle sizes both increase. When embryonic zeolites are converted to ZSM-5 crystals, the bulky TiPBz reactant loses access to the catalytic sites

located inside the micropore volume and probes only those on the external surface of the growing crystals and the remaining embryos.

Another message from the catalytic tests is that these embryonic zeolites are thermally stable as they survive at 460°C calcination prior to their evaluation. When treated under much harsher conditions (800°C for 1 h under air), HT-100-12 still displays a noticeable catalytic activity, **Figure 7b**.

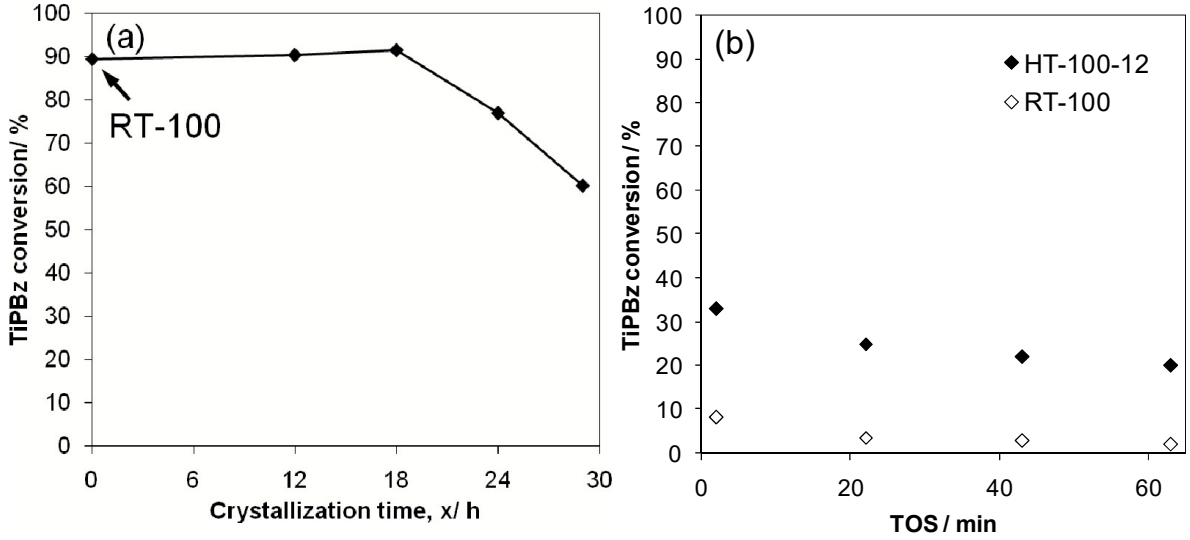

Figure 7: TiPBz conversion of (a) HT-100-x precursors after TOS=2 min, (b) HT-100-12 and RT-100 calcined at 800°C. Conditions: $T_{reaction}$=300°C, WHSV=8 h^{-1}. *Note: The HT-100-x precursor at x=0 h or without crystallization (i.e. HT-100-0) is RT-100.*

It could be also speculated that they can survive many regeneration cycles and may even be easier to regenerate as demonstrated recently for hierarchical ZSM-5 catalyts.[16]

Conclusions

Precursors of a ZSM-5, prepared in alkali metal free TPAOH-containing mixtures, show interesting textural properties reminiscent of amorphous silica-aluminas. When prepared at room temperature, these "embryonic zeolites", display micropores with diameters in the range of ZSM-5 zeolites. The absence of long range order implies a structure with dimensions lower than crystalline nano-sized ZSM-5. The combination of zeolite-like tetrahedrally coordinated aluminum (leading to Brønstedt acidity) and a micro-mesoporous texture (1-3 nm, allowing high accessibility to these acid sites) leads to catalysts with high activity in the dealkylation of TiPBz.

A subsequent controlled hydrothermal treatment of these embryonic zeolites leads to a substantial improvement in their catalytic activity and thermal stability. These embryonic zeolites show higher micropore accessibility than their zeolite offsprings and this suggests their potential use as catalysts, particularly in the conversion of heavy oil or very polar molecules.

Acknowledgments

This work was made possible by a PhD grant (KGH) from Total Raffinage Marketing. One of us (JPG) sincerely thanks the St-Nikon Foundation for continuous support. VV acknowledges the financial support from contract ANR-12-IS08-0001-01 (MicroGreen).

References

1. W. Vermeiren and J.-P. Gilson, *Top. Catal.*, 2009, **52**, 1131.
2. E. T. C. Vogt, G. T. Whiting, A. D. Chowdhury and B. M. Weckhuysen, *Adv. Catal.*, 2015, **58**, 143.
3. A. Corma, *Chem. Rev.*, 1997, **97**, 2373.
4. S. van Donk, A. H. Janssen, J. H. Bitter and K. P. de Jong, *Catal. Rev. Sci. Eng.*, 2003, **45**, 297.
5. M. Hartmann, *Angew. Chem. Int. Ed.*, 2004, **43**, 5880.
6. B. F. Chmelka, *Nat. Mater.*, 2006, **5**, 681.
7. R. F. Lobo, *Nature*, 2006, **443**, 757.
8. Y. Tao, H. Kanoh, L. Abrams and K. Kaneko, *Chem. Rev.*, 2006, **106**, 896.
9. J. Čejka and S. Mintova, *Catal. Rev. Sci. Eng.*, 2007, **49**, 457.
10. V. Meynen, P. Cool and E. F. Vansant, *Microporous Mesoporous Mater.*, 2007, **104**, 26.
11. K. Egeblad, C. H. Christensen, M. Kustova and C. H. Christensen, *Chem. Mater.*, 2008, **20**, 946.
12. J. Pérez-Ramírez, C. H. Christensen, K. Egeblad, C. H. Christensen and J. C. Groen, *Chem. Soc. Rev.*, 2008, **37**, 2530.
13. R. Chal, C. Gérardin, M. Bulut and S. van Donk, *ChemCatChem*, 2011, **3**, 67.

14. F. C. Meunier, D. Verboekend, J.-P. Gilson, J. C. Groen and J. Pérez-Ramírez, *Microporous Mesoporous Mater.*, 2012, **148**, 115.
15. F. Ngoye, L. Lakiss, Z. Qin, S. Laforge, C. Canaff, M. Tarighi, V. Valtchev, K. Thomas, A. Vicente, J.-P. Gilson, Y. Pouilloux, C. Fernandez and L. Pinard, *J. Catal.*, 2014, **320**, 118.
16. L. Lakiss, F. Ngoye, C. Canaff, S. Laforge, Y. Pouilloux, Z. Qin, M. Tarighi, K. Thomas, V. Valtchev, A. Vicente, L. Pinard, J.-P. Gilson and C. Fernandez, *J. Catal.*, 2015, **328**, 165.
17. G. Bellussi, C. Perego, A. Carati, S. Peratello, E. Previde Massara and G. Perego, in *Stud. Surf. Sci. Catal.*, Elsevier, 1994, **84**, 85.
18. M. R. S. Manton and J. C. Davidtz, *J. Catal.*, 1979, **60**, 156.
19. P. A. Jacobs, E. G. Derouane and J. Weitkamp, *J.C.S. Chem. Comm.*, 1981, 591.
20. W. D. Harkins and G. Jura, *J. Chem. Phys.*, 1943, **11**, 431.
21. E. P. Barrett, L. S. Joyner and P. P. Halenda, *J. Am. Chem. Soc.*, 1951, **73**, 373.
22. P. Tarazona, *Phys. Rev. A.*, 1985, **31**, 2672.
23. P. Tarazona, *Phys. Rev. A.*, 1985, **32**, 3148.
24. P. Tarazona, U. M. B. Marconi and R. Evans, *Mol. Phys.*, 1987, **60**, 573.
25. C. Rizzo, A. Carati, C. Barabino, C. Perego and G. Bellussi, in *Stud. Surf. Sci. Catal.*, Elsevier, 2001, **140**, 401.
26. P.-P. E. A. De Moor, T. P. M. Beelen, B. U. Komanshek, O. Diat and R. A. van Santen, *J. Phys. Chem. B.*, 1997, **101**, 11077.
27. P.-P. E. A. De Moor, T. P. M. Beelen, B. U. Komanschek, L. W. Beck, P. Wagner, M. E. Davis and R. A. van Santen, *Chem.-Eur. J.*, 1999, **5**, 2083.
28. C. E. A. Kirschhock, R. Ravishankar, F. Verspeurt, P. J. Grobet, P. A. Jacobs and J. A. Martens, *J. Phys. Chem. B.*, 1999, **103**, 4965.
29. R. Ravishankar, C. E. A. Kirschhock, P-P. Knops-Gerrits, E. J. P. Feijen, P. J. Grobet, P. Vanoppen, F. C. De Schryver, G. Miehe, H. Fuess, B. J. Schoeman, P. A. Jacobs and J. A. Martens, *J. Phys. Chem. B.*, 1999, **103**, 4960.
30. C. E. A. Kirschhock, R. Ravishankar, L. van Looveren, P. A. Jacobs and J. A. Martens, *J. Phys. Chem. B.*, 1999, **103**, 4972.
31. C. E. A. Kirschhock, R. Ravishankar, P. A. Jacobs and J. A. Martens, *J. Phys. Chem. B.*, 1999, **103**, 11021.

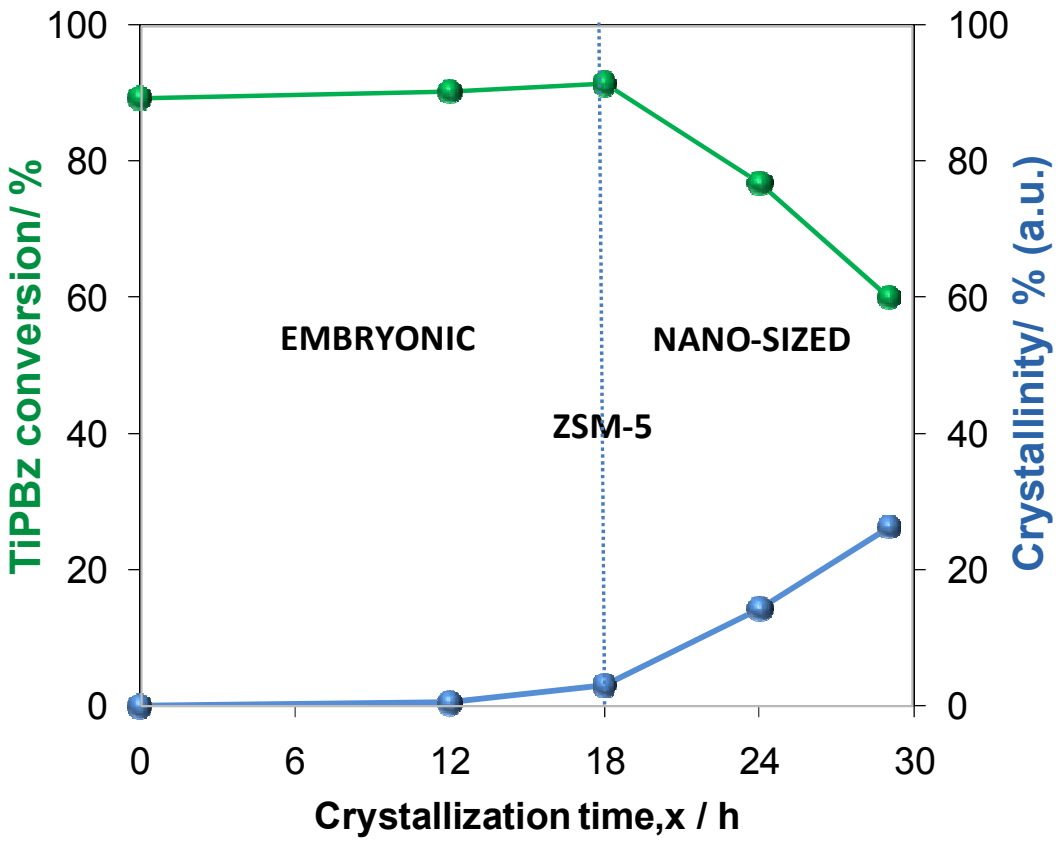

Embryonic ZSM-5's have more accessible microporosity than their zeolite offsprings and are therefore better catalysts to convert bulky molecules.